Preprints.org

Article

Not peer-reviewed version

Imaging Characteristics of Hypervascular Focal Nodular Hyperplasia-Like Lesions in Patients with Chronic Alcoholic Liver Disease

Atsushi Urase , Masakatsu Tsurusaki * , Ryohei Kozuki , Atsushi Kono , Keitaro Sofue , Kazunari Ishii

Posted Date: 20 December 2023

doi: 10.20944/preprints202312.1508.v1

Keywords: focal nodular hyperplasia; alcoholic liver disease; hepatocellular carcinoma; magnetic resonance imaging

Preprints.org is a free multidiscipline platform providing preprint service that is dedicated to making early versions of research outputs permanently available and citable. Preprints posted at Preprints.org appear in Web of Science, Crossref, Google Scholar, Scilit, Europe PMC.

Copyright: This is an open access article distributed under the Creative Commons Attribution License which permits unrestricted use, distribution, and reproduction in any medium, provided the original work is properly cited.

Preprints (www.preprints.org) | NOT PEER-REVIEWED | Posted: 20 December 2023 doi:10.20944/preprints202312.1508.v1

Disclaimer/Publisher's Note: The statements, opinions, and data contained in all publications are solely those of the individual author(s) and contributor(s) and not of MDPI and/or the editor(s). MDPI and/or the editor(s) disclaim responsibility for any injury to people or property resulting from any ideas, methods, instructions, or products referred to in the content.

Article

Imaging Characteristics of Hypervascular Focal Nodular Hyperplasia-Like Lesions in Patients with Chronic Alcoholic Liver Disease

Atsushi Urase [1,#], Masakatsu Tsurusaki [1,*,#], Ryohei Kozuki [1], Atsushi Kono [1], Keitaro Sofue [2] and Kazunari Ishii [1]

[1] Department of Radiology, Kindai University, Faculty of Medicine, Osakasayama, 589-8511 Japan; 1979c9@med.kindai.ac.jp (A.U.); mtsuru@dk2.so-net.ne.jp (M.T.); kozuki1023rp@gmail.com (R.K.); ringonotegami@mac.com (A.K.); ishii@med.kindai.ac.jp (K.I.)

[2] Department of Radiology, Kobe University, Graduate School of Medicine, Kobe, 650-0017 Japan; keitarosofue@yahoo.co.jp (K.S.)

* Correspondence: author: mtsuru@dk2.so-net.ne.jp; Tel.: +81 (72) 366-0221; Fax: +81 (72) 366-0206

[#] Atsushi Urase and Masakatsu Tsurusaki equally contributed to the study and should be considered as co-first authors of this study.

Simple Summary: Focal nodular hyperplasia (FNH)-like lesions have unique radiological findings, including superparamagnetic iron oxide- and/or gadoxetic acid-enhanced magnetic resonance imaging (MRI) and computed tomography (CT) during hepatic angiography features, which can facilitate their differential diagnosis from hepatocellular carcinoma. In this study, the uptake of liver-specific MR contrast agents was observed in all FNH-like lesions. Furthermore, MRI and hypervascularity on CT were useful for the diagnosis of FNH-like lesions.

Abstract: We evaluated diagnostically differential radiological findings between focal nodular hyperplasia (FNH)-like lesions and hepatocellular carcinoma (HCC). We studied pathologically confirmed FNH-like lesions in 13 alcoholic-cirrhosis patients who were negative for hepatitis-B surface antigen and hepatitis-C virus antibody and underwent dynamic computed tomography (CT) and magnetic resonance imaging (MRI), including superparamagnetic iron oxide (SPIO) and/or gadoxetic acid-enhanced MRI. Seven patients underwent angiography-assisted CT. Evaluated lesion features included arterial enhancement pattern, washout appearance (low density compared to surrounding liver parenchyma), signal intensity on T1-weighted image (T1WI) and T2-weighted image (T2WI), central scar presence, chemical shift on in- and out-of-phase images, and uptake pattern on gadoxetic acid-enhanced MRI hepatobiliary phase and on SPIO-enhanced MRI. Eleven patients had multiple small lesions (<1.5 cm). Radiological features of FNH-like lesions included hypervascularity despite small lesion, lack of "corona-like" enhancement in the late phase on CT during hepatic angiography (CTHA), high-intensity on T1WI, slightly high- or iso-intensity on T2WI, no signal decrease in out-of-phase images, and complete SPIO uptake or incomplete/partial uptake of gadoxetic acid. Pathologically, like HCC, FNH-like lesions showed many unpaired arteries and sinusoidal capillarization. In summary, FNH-like lesions have unique radiological findings useful for differential diagnosis. Specifically, SPIO- and/or gadoxetic acid-enhanced MRI and CTHA features might facilitate differential diagnosis of FNH-like lesions and HCC.

Keywords: focal nodular hyperplasia; alcoholic liver disease; hepatocellular carcinoma; magnetic resonance imaging

1. Introduction

Since Glund et al. [1] reported the development of hyperplastic lesions during the follow-up period in patients with micronodular cirrhosis and a history of alcohol abuse, other studies have reported hyperplastic lesions in patients with alcoholic liver cirrhosis [2–7]. These lesions have several pathological similarities to focal nodular hyperplasia (FNH) in non-cirrhotic livers; therefore,

© 2023 by the author(s). Distributed under a Creative Commons CC BY license.

Preprints (www.preprints.org) | NOT PEER-REVIEWED | Posted: 20 December 2023 doi:10.20944/preprints202312.1508.v1

they are currently termed as FNH-like lesions or nodules. However, FNH-like lesions in alcoholic liver cirrhosis are yet to be described in the International Working Party [8] and World Health Organisation (WHO) [7] classifications for hepatocytic lesions. Nakajima et al. [7] reported that FNH-like lesions are characterized by hypervascularity caused by scar-like fibrosis with anomalous blood vessels and unpaired arteries. Moreover, they reported difficulty in distinguishing hyperplastic lesions from well-differentiated hepatocellular carcinoma (HCC) in their biopsy cases. Similarly, hypervascularity is observed in most cases of HCC. Only few studies have described the radiological findings of FNH-like lesions [8], which could be attributed to their rarity. Quaglia et al. [4] reported that 5% of distinctive nodular lesions in explant cirrhotic livers had FNH-suggestive features. Moreover, Libbrecht et al. [6] reported five FNH-like nodules in 4 (8%) out of 49 cirrhotic explant livers. In this study, we aimed to describe the clinical and radiological characteristics of FNH-like lesions in patients with alcoholic liver cirrhosis using multiple modalities.

2. Materials and methods

2.1. Patients

This retrospective study was approved by the institutional ethics committee of xxx University, Faculty of Medicine. All patients provided informed consent for the use of their computed tomography (CT) and magnetic resonance (MR) images as well as biopsy specimens. The study protocol conformed to the ethics guidelines of the 2002 Declaration of Helsinki.

We included 13 patients with pathologically confirmed FNH-like lesions who underwent dynamic CT, unenhanced MR imaging (I), and superparamagnetic iron oxide (SPIO)- and/or gadoxetic acid-enhanced MRI between 2000 and 2020. In all the patients, liver cirrhosis was determined through clinical examination and blood chemistry tests (for aspartate aminotransferase, alanine aminotransferase, alkaline phosphatase, bilirubin, albumin, and globulin). Further, each patient had at least one FNH-like nodule pathologically diagnosed through biopsy, with the remaining lesions being diagnosed based on clinical findings indicating no decrease in size after abstinence from alcohol during the 1-year follow up.

2.2. Imaging technique

Plain and three-phase contrast-enhanced CT scans were obtained in a craniocaudal direction using Sensation 64 CT (Siemens, Erlangen, Germany) or Aquilion multi 64 (Canon Medical System, Otawara, Japan) scanners. Routine scanning was conducted at a 5-mm section thickness and 5-mm scan increment. Subsequently, the scans were reconstructed with a 2-mm thickness using a routine abdominal algorithm. An injector system was used to intravenously administer 100–150 ml non-ionic contrast media (Iopamiron®; 300/370 mgI/ml; Bayer Schering Pharma, Berlin, Germany) at a rate of 3–3.5 ml/s.

All MRIs were performed on a 1.5-T system using the Magnetom Avanto (Siemens Healthcare, Erlangen, Germany) or Signa HDxt (GE Healthcare, Waukesha, WI, USA) scanner. Baseline MR images were acquired using a respiratory-triggered T2-weighted turbo spin-echo (TSE) sequence, breath-hold T2*-weighted gradient-echo (GRE) imaging with steady-state precession (FISP) sequence, and breath-hold T1-weighted GRE sequence. All images were obtained in the transaxial plane using a phased-array multi-coil. For all sequences, a 7-mm slice thickness was used, with a 10% intersection gap and a field of view of 35–40 cm, depending on the liver size. SPIO-enhanced MRI comprised the respiratory-triggered T2-TSE sequence, breath-hold T2*-weighted FISP sequence, and breath-hold T1-weighted GRE sequence, with the same parameters as those used in baseline MRI. Fercarbotran (Resovist®; Bayer Yakuhin, Osaka, Japan) at a dose of 8.0 μmol iron per kg (body weight) was manually injected as a rapid bolus through a filter with 5-μm pore size, which was immediately followed by a 10 ml saline solution flush. Imaging was then performed after 7 minutes. Gadoxetic acid-enhanced MRI comprised dynamic images constructed using fat-suppressed T1-weighted GRE images obtained before (pre-contrast) as well as 14–30 s (arterial phase), 70 s, and 3 min after intravenous administration of 0.025 mmol of gadoxetic acid (Primovist®, Bayer Schering

Preprints (www.preprints.org) | NOT PEER-REVIEWED | Posted: 20 December 2023 doi:10.20944/preprints202312.1508.v1

Pharma, Berlin, Germany) per kg (body weight) at a rate of 2.0 ml/s, followed by a 20 ml saline flush. Hepatobiliary phase (HBP) images were obtained 20 min after gadoxetic acid injection.

All CTAP and double-phase CT during hepatic angiography (CTHA) examinations were performed using a unified angiography and CT system (Multistar Plus/Somatom Plus 4 Volume Zoom; Siemens, Erlangen, Germany). These images were obtained in a craniocaudal direction with 5-mm section thickness and 5-mm reconstruction intervals. For double-phase CTHA, first-phase data acquisition was started 5 s after second-phase data acquisition, which was performed 21 s–26 s after initiation of a transcatheter hepatic arterial injection of a fixed dose of 20 ml iohexol (Omnipaque 300, 300 mgI/ml; Daiichi-Sankyo Parma, Tokyo, Japan) diluted with 33% sterile water (iodine, 100 mg iodine/ml) at a rate of 2 ml/s.

2.3. Pathological analysis

All patients underwent ultrasound-guided core needle biopsy. All liver samples were fixed in 10% neutral-buffered formalin, routinely processed for paraffin embedding, sectioned (4 μm), and stained with hematoxylin and eosin. Immunohistochemical analysis was performed using seven patient samples.

2.4. Image analysis

Two radiologists (M.T. and K.S.) with > 10 years of experience evaluated the following lesion characteristics: the number and size (largest axial diameter) of each lesion; dynamic enhancement pattern on dynamic CT and CTHA (a–b) for qualitative imaging analysis; and other MRI features (c–h) as follows: (a) arterial enhancement pattern of the dynamic CT and/or first phase of the CTHA, (b) washout appearance (defined as low density compared with the density of the surrounding liver parenchyma) on the portal venous phase (PVP) of the dynamic CT and/or second phase of the CTHA, (c) signal intensity on T1-weighted image (T1WI), (d) signal intensity on T2-weighted image (T2WI), (e) central scar (defined as a central T2 hyperintensity and/or T1 hypointensity representing fibrotic tissue), (f) chemical shift (defined as a drop in signal intensity on out-of-phase images compared with that on in-phase images), (g) uptake pattern on the HBP of the gadoxetic acid-enhanced MRI, and (h) uptake pattern on the SPIO-enhanced MRI. Arterial enhancement was classified as homogeneous (peripherally or entirely) or heterogeneous. Signal intensity on T1WIs was classified as hypointensity, iso- or hyperintensity, or heterogeneous signal intensity. Signal intensity on T2WIs was classified as iso-intensity or hyperintensity. Uptake on the HBP of gadoxetic acid- and SPIO-enhanced MRI was classified as homogeneous (peripherally or entirely) or heterogeneous. In case of interobserver discordance, the radiologists re-evaluated the images and reached a consensus. Both radiologists were informed about the location of each lesion; however, they were blinded to the clinical information and final diagnosis.

3. Results

We included 13 patients (10 men and 3 women; mean age: 54.5 ± 12.5 [33–72] years) with chronic liver failure due to alcoholic liver disease. Table 1 shows a summary of the clinical findings. All patients with FNH-like lesions were pathologically diagnosed using fine-needle biopsy. The levels of alpha-fetoprotein (AFP) and prothrombin induced by vitamin K deficiency or antagonist-II were normal in all patients with FNH-like lesions except for one patient with HCC who had elevated AFP levels. Among the 10 patients with FNH-like lesions, 2 (20%) showed new lesions after abstinence from alcohol. The size of the FNH-like lesions remained stable or decreased in eight (80%) patients.

Table 1. Summary of clinical findings.

Patient no.	Age (y)	Sex	Background of liver failure	Child Pugh grade	AFP	PIVKA-II	Diagnosis	Lesion growth at imaging follow up
1	41	M	Alcoholic	A	6	23	FNB	N/A

Preprints (www.preprints.org) | NOT PEER-REVIEWED | Posted: 20 December 2023 doi:10.20944/preprints202312.1508.v1

2	33	F	Alcoholic	A	7	23	FNB	No growth
3	34	F	Alcoholic	B	4	10	FNB	Increased number
4	60	M	Alcoholic	B	9	20	FNB	No growth
5	58	M	Alcoholic	A	7	40	FNB	No growth
6	57	M	Alcoholic	B	6	19	FNB	N/A
7	53	M	Alcoholic	B	23*	33	FNB	No growth
8	65	M	Alcoholic	A	10	18	FNB	Increased number
9	63	M	Alcoholic	A	6	12	FNB	No growth
10	48	F	Alcoholic	B	11	18	FNB	No growth
11	55	M	Alcoholic	B	5	16	FNB	N/A
12	70	M	Alcoholic	A	5	22	FNB	No growth
13	72	F	Alcoholic	A	4	15	FNB	No growth

* Case 7 was only the patient with HCCs. FNB = fine needle biopsy, N/A = not available.

Table 2 shows the CT findings of the FNH-like lesions. Among the 13 patients with 26 FNH-like lesions, seven had a single lesion while six had multiple lesions (two, one, and three patients had two, three, and over four lesions, respectively). The lesion size ranged from 10 mm to 30 mm (mean ± standard deviation, 14.0 ± 5.5 mm). All 26 FNH-like lesions exhibited marked hypervascularity during the arterial phase on contrast-enhanced CT (CE-CT) and CTHA (seven patients) as well as wash-out appearance during the portal venous and equilibrium phases on CE-CT. Pathological examination revealed numerous unpaired arteries and sinusoidal capillarization in all patients, which were similar to those in HCC.

Table 2. Summary of tumor characteristics, dynamic patterns assessed using CT and CTHA, and pathological findings.

Patient no.	No. of nodules	Size	Arterial enhancement pattern	Washout appearance	Modality	Central scar	Unpaired arteries and capillarization	Liver cell atypia	Scar-like fibrosis
1	2	15	hyper	no	CECT/CTHA	-	+	-	-
2	1	15	hyper	no	CECT/CTHA	-	+	-	-
3	>4	10–15	hyper	no	CECT/CTHA	-	+	-	-
4	>4	10–30	hyper	no	CECT/CTHA	+	+	-	+
5	1	10	hyper	no	CECT	-	+	-	-
6	3	10–30	hyper	no	CECT/CTHA	-	+	-/+	-
7	1	15	hyper	no	CECT/CTHA	+	+	-	+
8	1	10	hyper	no	CECT	-	+	-	-
9	1	10	hyper	no	CECT	-	+	-	-
10	>4	10–15	hyper	no	CECT/CTHA	-	+	-	-
11	2	15	hyper	no	CECT	-	+	-	-

Preprints (www.preprints.org) | NOT PEER-REVIEWED | Posted: 20 December 2023 doi:10.20944/preprints202312.1508.v1

12	1	20	hyper	no	CECT	-	+	-	-
13	1	14	hyper	no	CECT	+	+	-	-

CT, computed tomography; CECT, contrast-enhanced CT; CTHA, CT hepatic arteriography.

Table 3 shows the MRI findings of the FNH-like lesions. Among the thirteen patients with FNH-like lesions, eleven (85%) showed high or iso-high intensity on T1WI, seven (54%) showed iso-high intensity on T2WI, six (46%) showed low intensity, three (23%) showed high-intensity central scars, and 10 (77%) showed no central scars on T2WI. Chemical shift artefacts were observed in all the 13 patients with FNH-like lesions (Figures 1 and 2). In the six patients who underwent gadoxetic acid-enhanced MRI (Figures 3 and 4), all lesions exhibited marked homogeneous enhancement during the arterial phase. Two enhancement patterns were observed on the HBP: heterogeneous hyperintense (n = 3, 43%) and ring-like enhancement (n = 4, 57%). In the eight patients who underwent SPIO-enhanced MRI, all lesions exhibited a marked homogeneous uptake pattern on post-SPIO-enhanced MRI (Figures 1 and 3).

Table 3. Summary of MRI characteristics and findings.

Patient no.	T1-weighted images	T2-weighted images	Central scar on MR imaging	Chemical shift	Uptake pattern on the HBP	Uptake pattern on the SPIO
1	high	iso-high	no	no	N/A	homogenous
2	high	iso-high	no	no	N/A	N/A
3	high	low	no	no	N/A	homogenous
4	iso-high	low	yes	no	N/A	homogenous
5	high	Iso-high	no	no	ring	homogenous
6	low-high	low	no	no	N/A	homogenous
7	high	iso	yes	no	N/A	homogenous
8	high	low	no	no	ring/hetero	homogenous
9	high	iso-high	no	no	N/A	homogenous
10	high	iso-high	no	no	hetero	N/A
11	high	low	no	no	ring	N/A
12	iso	low	no	no	hetero	N/A
13	iso-high	iso-high	yes	no	ring	N/A

N/A = not available.

Preprints (www.preprints.org) | NOT PEER-REVIEWED | Posted: 20 December 2023 doi:10.20944/preprints202312.1508.v1

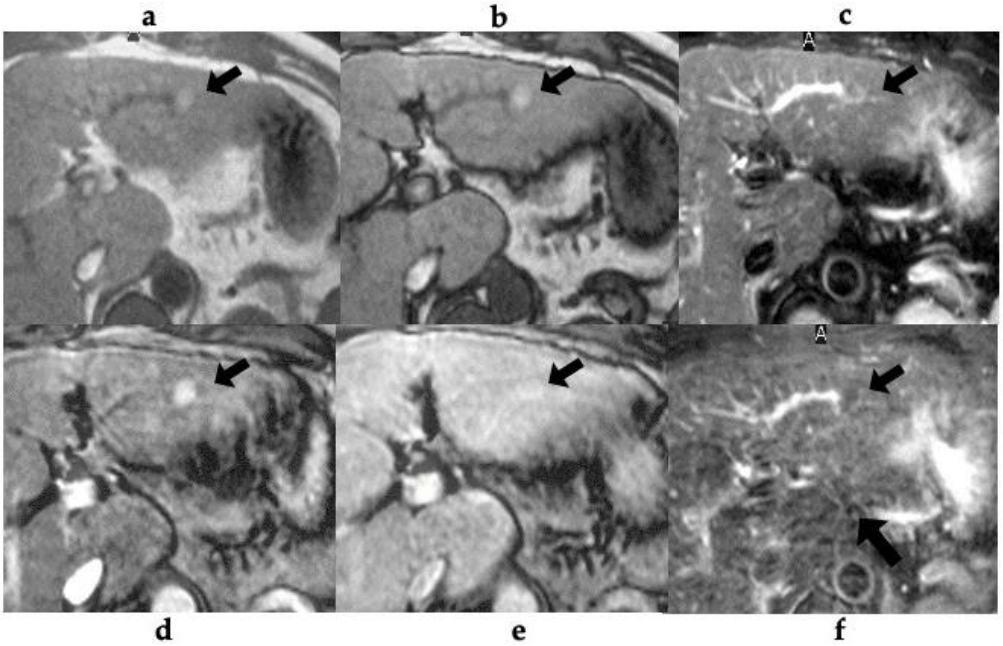

Figure 1. 58-year-old man with alcoholic liver cirrhosis (patient no. 5). **(a-b)** T1-weighted gradient-echo (GRE) MR (**a**; in-phase, **b**; opposed-phase) image shows a small and high-signal-intensity nodule (arrow) in the lateral segment. **(c)** T2-weighted fast spin-echo MR image shows iso intensity nodule (arrow). Gadolinium-enhanced T1-weighted GRE MR imaging obtained during the **(d)** arterial- and **(e)** portal-venous phase reveals a nodule with arterial phase hyperenhancement (arrow) and without washout (arrow). **(f)** The SPIO-enhanced T2*-weighted GRE MR image shows the lesion as a low-signal intensity nodule (arrow) with SPIO-uptake compared with the surrounding liver parenchyma.

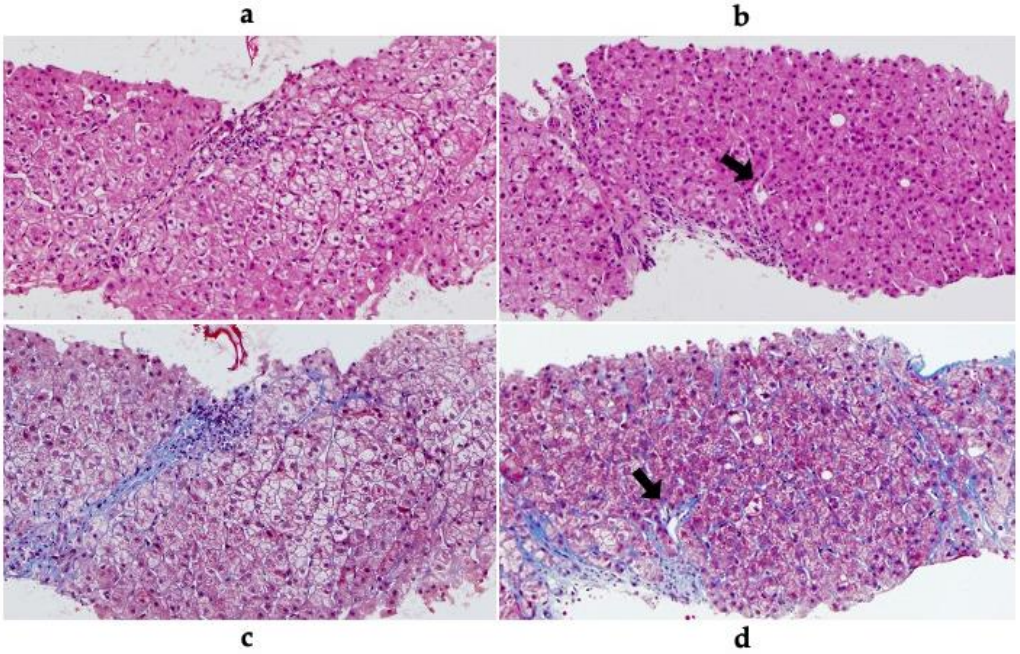

Figure 2. Histopathological features of non-nodular **(a, c)** and nodular **(b, d)** portions. **(a, c)** Chronic hepatitis with pericellular fibrosis and diffuse capillarization of the sinusoids probably due to alcoholic injury with mild activity and moderate fibrosis. (a: Hematoxylin and eosin staining ×100, c: Masson trichrome staining ×100). Histopathological features of the nodular portion. **(b, d)**

Preprints (www.preprints.org) | NOT PEER-REVIEWED | Posted: 20 December 2023 doi:10.20944/preprints202312.1508.v1

Hyperplastic nodule with a mild increase in cell density and pericellular fibrosis. There are some unpaired arteries (arrow) in the nodule (b: Hematoxylin and eosin staining ×100, d: Masson trichrome staining ×100).

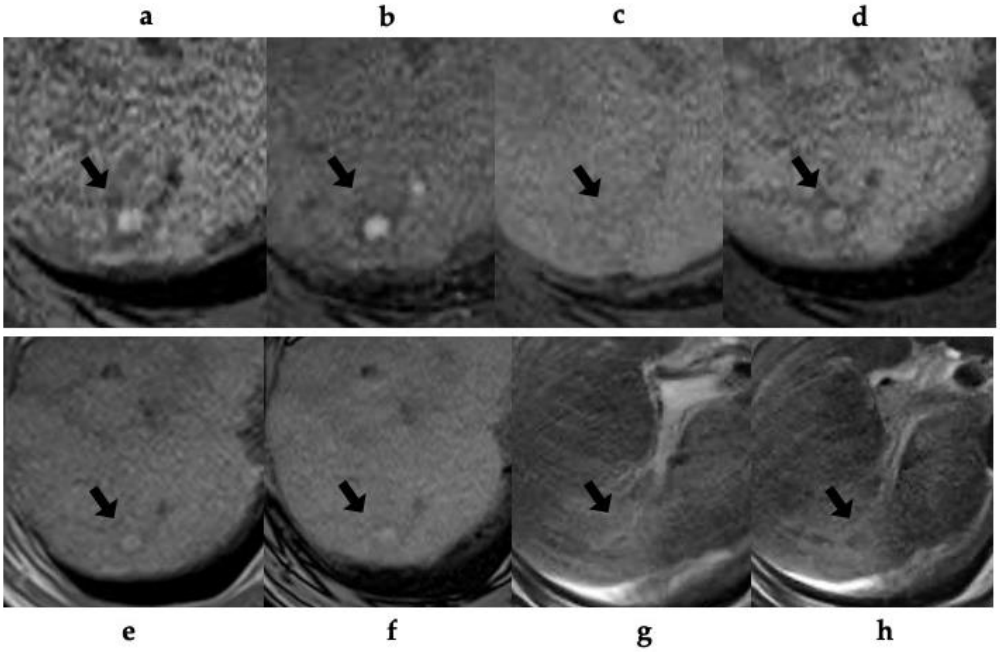

Figure 3. A 65-year-old man with alcoholic liver cirrhosis (patient no. 8). **(a-b)** T1-weighted gradient-echo (GRE) MR (**a**; in-phase, **b**; opposed-phase) image shows a small and high-signal-intensity nodule (arrow) in segment 7 of the liver. **(c)** pre-contrast T1-weighted GRE MR imaging shows iso-slightly high-intensity nodule (arrow). Gadoxetic acid-enhanced T1-weighted GRE MR imaging obtained during the **(d)** arterial- and **(e)** portal-venous phase reveal a nodule with arterial phase hyperenhancement (arrow) and without washout (arrow). **(f)** The hepatobiliary phase of the gadoxetic acid-enhanced T1-weighted GRE MRI shows homogeneous high-intense uptake (arrow). **(g)** T2*-weighted GRE MR image shows iso-intensity nodule (arrow). **(h)** The SPIO-enhanced T2*-weighted GRE MR image shows the lesion as a low-signal intensity nodule (arrow) with SPIO-uptake compared with the surrounding liver parenchyma.

Preprints (www.preprints.org) | NOT PEER-REVIEWED | Posted: 20 December 2023 doi:10.20944/preprints202312.1508.v1

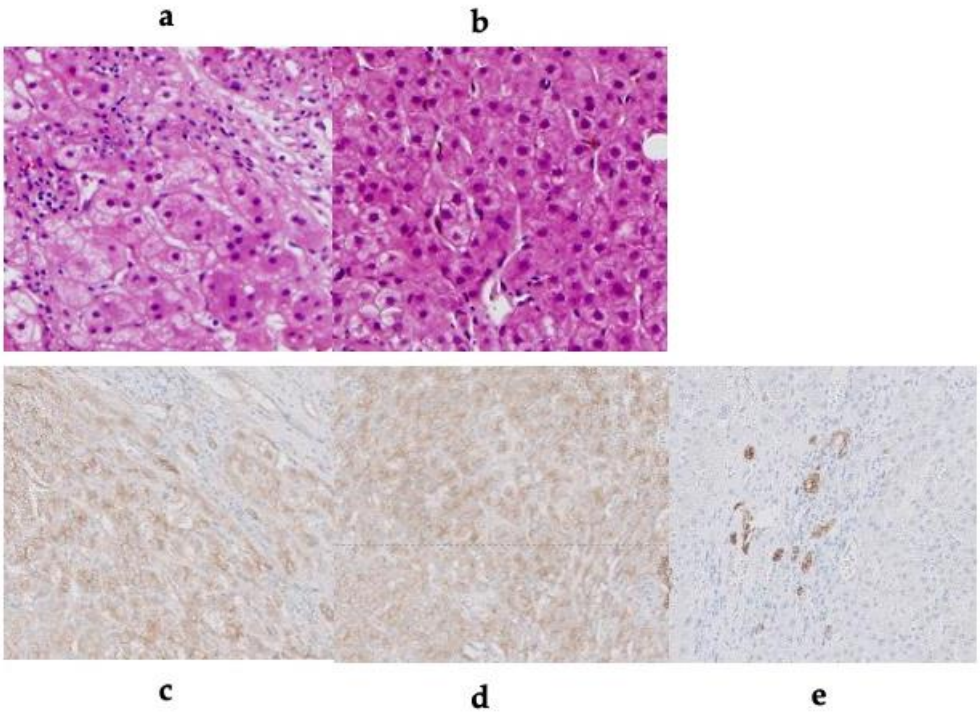

Figure 4. Histopathological features of the non-nodular **(a, c)** and nodular **(b, d)** portions. **(a, b)** Cell density, iron deposits, and sinusoidal capillarization in the surrounding liver tissue (a) and the FNH-like nodule (b). The FNH-like nodule shows increased cell density (a, hematoxylin and eosin staining ×400) **(c, d)** OATP8 (red-orange color) is expressed on the cellular membrane of hepatocytes at the sinusoidal side. The expression of OATP1B3 is nearly absent in the nodule (b, ×400); however, it is diffusely found in the surrounding tissue (c, ×400). OATP1B3 is immunohistochemically detected using anti-OATP1B3. (f) Immunohistochemical staining of CD68 antigen showing Kupffer cells. The staining of nodule CD68 antigen shows diffuse Kupffer cell infiltration.

4. Discussion

In this study, we studied pathologically confirmed FNH-like lesions in 13 patients with alcoholic cirrhosis. The radiological features of FNH-like lesions included hypervascularity despite small lesions, lack of "corona-like" enhancement in the late phase on CT during hepatic angiography (CTHA), high-intensity on T1WI, slightly high- or iso-intensity on T2WI, no signal decrease in out-of-phase images, and complete SPIO uptake or incomplete/partial uptake of gadoxetic acid.

There have been several recent reports of FNH-like lesions in cirrhotic livers [1–6]. Although there remains no established definition for an FNH-like lesion/nodule, FNH is known to develop in normal livers. Accordingly, FNH–like lesions refer to similar nodules observed in patients with chronic liver disease [7]. These lesions have been extensively reported in alcoholic liver disease [8,9]. Most of these hyperplastic lesions are highly vascular and relatively small-sized; additionally, they are difficult to differentiate from HCC lesions, especially early-stage HCC lesions [7–9]. We included 13 patients with alcoholic liver disease and hyperplastic liver lesions who were negative for hepatitis virus markers. Here, we discuss the imaging findings with respect to reported imaging characteristics of such lesions [10–14].

In our cases, except for a normal hepatic background and absence of a central scar, the pathological findings were consistent with those of FNH; accordingly, the patients were diagnosed with FNH-like lesions based on the original text in the WHO classification (version 5) [15]. There has been no previous report on the radiographic findings of FNH-like lesions based on our exact definition since there remains no established definition. However, considering the similarities of the histopathology and imaging findings with those of FNH, it is highly likely that FNH–like lesions have been previously described as atypical FNH based on imaging findings. Approximately 80% of

Preprints (www.preprints.org) | NOT PEER-REVIEWED | Posted: 20 December 2023 doi:10.20944/preprints202312.1508.v1

FNH cases are reported to be atypical on imaging [16]. Typical FNH on plain CT is characterized by hypo- to iso-attenuation, with homogeneous attenuation in early-phase contrast enhancement and isoattenuation with the surrounding liver from the PVP to the equilibrium phase. On MRI, these lesions present as iso- to moderately hypointense on T1WIs, iso- to somewhat hyperintense on T2WIs, and iso- to somewhat hyperintense or ring-like hyperintense in the hepatocyte phase after gadoxetic acid-enhanced MR imaging [10–14,17]. The central scar is hypointense on plain CT and early-phase contrast enhancement CT, with delayed enhancement into the equilibrium phase. Additionally, the central scar is hypointense on T1WIs and hyperintense on T2WIs; further, the region, including the surrounding area, has low uptake of gadoxetic acid during the hepatocyte phase. However, a central scar is only observed in approximately 50% of cases [18].

Single-level dynamic CTHA has indicated that blood flows from a dilated feeding artery inside the central scar; moreover, blood within the lesion directly flows into the hepatic vein via the fibrous septum and dilated veins at the margin of the lesion [19]. Grazioli et al. [17] did not report the imaging characteristics of six nodules with hypointense enhancement; therefore, it remains unclear whether there was a complete lack of enhancement. Notably, the enhancement was relatively lower than that of the surrounding liver; moreover, the heterogeneity was similar to that in our cases; however, their nodules exhibited overall hypointense enhancement. In addition, similar to our cases, the nodule lacked a central scar. Furthermore, although there is heterogeneity in the signal intensity in the hepatocyte phase of typical FNH, which ranges from iso- to hyperintense enhancement, the mechanisms underlying these findings remain unclear. Moreover, the cause of the relatively low enhancement in the uptake area within the nodule remains unclear.

This study has several limitations. First, this retrospective study had inevitable selection bias. Additionally, all patients with FNH-like lesions were pathologically confirmed using fine-needle biopsy specimens rather than surgical specimens. Finally, there was no standard follow-up imaging of the FNH-like lesions; further, we did not describe the frequency of this phenomenon. Further large-scale multicenter studies using surgical specimens are warranted.

4. Conclusions

The radiological features of FNH-like lesions in patients with chronic alcoholic liver disease are as follows: (1) small lesion (approximately < 1.5 cm); (2) high signal intensity on T1WIs; (3) no chemical shift effect (no signal intensity decrease on opposed phase); (4) uptake of SPIO or gadoxetic acid; and (5) hypervascularity despite the small-sized lesion. Pathologically, FNH-like lesions present a high number of unpaired arteries and sinusoidal capillarization, which may mimic HCC. It is important to identify differential radiological, pathological, and clinical findings between FNH-like nodules and HCC.

Author Contributions: Conceptualization: M.T.; methodology: M.T.; formal analysis: A.U.; image analysis: A.U., M.T., and K.S.; data curation: A.U., M.T., R.K., T.K., A.K., and K.S.; writing—original draft preparation: A.U. and M.T.; writing—review and editing: M.T.; supervision: K.I. All authors have read and agreed to the published version of the manuscript. Atsushi Urase and Masakatsu Tsurusaki have equally contributed to the study and should be considered as co-first authors of this study.

Funding: This research received no external funding.

Institutional Review Board Statement: This retrospective study was performed with the approval of the institutional ethics committee of the Faculty of Medicine, Kindai University.

Informed Consent Statement: Informed consent for using their computed tomography (CT) and magnetic resonance (MR) images and biopsy specimens was obtained from all patients.

Data Availability Statement: The data presented in this study are available on request from the corresponding author. The data are not publicly available owing to privacy.

Acknowledgments: We would like to thank Editage (www.editage.com) for English language editing.

Conflicts of Interest: The authors declare no conflict of interest.

Preprints (www.preprints.org) | NOT PEER-REVIEWED | Posted: 20 December 2023 doi:10.20944/preprints202312.1508.v1

References

1. Gluud, C.; Christoffersen, P.; Eriksen, J.; Wantzin, P.; Knudsen, B. B. Influence of Ethanol on Development of Hyperplastic Nodules in Alcoholic Men with Micronodular Cirrhosis. *Gastroenterology* **1987**, *93*, 256–260. DOI: 10.1016/0016-5085(87)91011-0
2. Sugihara, S.; Nakashima, O.; Kiyomatsu, K.; Ijiri, M.; Edamitsu, O.; Kojiro, M. A Case of Liver Cirrhosis with a Hyperplastic Nodular Lesion. *Acta Pathol. Jpn.* **1990**, *40*, 699–703. DOI: 10.1111/j.1440-1827.1990.tb01619.x
3. Terada, T.; Kitani, S.; Ueda, K.; Nakanuma, Y.; Kitagawa, K.; Masuda, S. Adenomatous Hyperplasia of the Liver Resembling Focal Nodular Hyperplasia in Patients with Chronic Liver Disease. *Virchows Arch. A Pathol. Anat. Histopathol.* **1993**, *422*, 247–252. DOI: 10.1007/BF01621809
4. Quaglia, A.; Tibballs, J.; Grasso, A.; Prasad, N.; Nozza, P.; Davies, S. E.; Burroughs, A. K.; Watkinson, A.; Dhillon, A. P. Focal Nodular Hyperplasia-Like Areas in Cirrhosis. *Histopathology* **2003**, *42*, 14–21. DOI: 10.1046/j.1365-2559.2003.01550.x
5. An, H. J.; Illei, P.; Diflo, T.; John, D.; Morgan, G.; Teperman, L.; Theise, N. Scirrhous Changes in Dysplastic Nodules Do Not Indicate High-Grade Status. *J. Gastroenterol. Hepatol.* **2003**, *18*, 660–665. DOI: 10.1046/j.1440-1746.2003.03052.x
6. Libbrecht, L.; Bielen, D.; Verslype, C.; Vanbeckevoort, D.; Pirenne, J.; Nevens, F.; Desmet, V.; Roskams, T. Focal Lesions in Cirrhotic Explant Livers: Pathological Evaluation and Accuracy of Pretransplantation Imaging Examinations. *Liver Transpl.* **2002**, *8*, 749–761. DOI: 10.1053/jlts.2002.34922
7. Nakashima, O.; Kurogi, M.; Yamaguchi, R.; Miyaaki, H.; Fujimoto, M.; Yano, H.; Kumabe, T.; Hayabuchi, N.; Hisatomi, J.; Sata, M.; Kojiro, M. Unique Hypervascular Nodules in Alcoholic Liver Cirrhosis: Identical to Focal Nodular Hyperplasia-Like Nodules? *J. Hepatol.* **2004**, *41*, 992–998. DOI: 10.1016/j.jhep.2004.08.014
8. International Working Party. Terminology of Nodular Hepatocellular Lesions. *Hepatology* **1995**, *22*, 983–993. DOI: 10.1016/0270-9139(95)90324-0
9. Lee, Y. H.; Kim, S. H.; Cho, M. Y.; Shim, K. Y.; Kim, M. S. Focal Nodular Hyperplasia-Like Nodules in Alcoholic Liver Cirrhosis: Radiologic-Pathologic Correlation. *A.J.R. Am. J. Roentgenol.* **2007**, *188*, W459–W463. DOI: 10.2214/AJR.05.1998
10. Yoneda, N.; Matsui, O.; Kitao, A.; Kita, R.; Kozaka, K.; Koda, W.; Kobayashi, S.; Gabata, T.; Ikeda, H.; Sato, Y.; Nakanuma, Y. Hepatocyte Transporter Expression in FNH and FNH-Like Nodule: Correlation with Signal Intensity on Gadoxetic Acid Enhanced Magnetic Resonance Images. *Jpn. J. Radiol.* **2012**, *30*, 499–508. DOI: 10.1007/s11604-012-0085-4
11. Fujiwara, H.; Sekine, S.; Onaya, H.; Shimada, K.; Mikata, R.; Arai, Y. Ring-Like Enhancement of Focal Nodular Hyperplasia with Hepatobiliary-Phase Gd-EOB-DTPA-Enhanced Magnetic Resonance Imaging: Radiological-Pathological Correlation. *Jpn. J. Radiol.* **2011**, *29*, 739–743. DOI: 10.1007/s11604-011-0624-4
12. Mohajer, K.; Frydrychowicz, A.; Robbins, J. B.; Loeffler, A. G.; Reed, T. D.; Reeder, S. B. Characterization of Hepatic Adenoma and Focal Nodular Hyperplasia with Gadoxetic Acid. *J. Magn. Reson. Imaging* **2012**, *36*, 686–696. DOI: 10.1002/jmri.23701
13. Grieser, C.; Steffen, I. G.; Kramme, I. B.; Bläker, H.; Kilic, E.; Perez Fernandez, C. M.; Seehofer, D.; Schott, E.; Hamm, B.; Denecke, T. Gadoxetic Acid Enhanced MRI for Differentiation of FNH and HCA: A Single Centre Experience. *Eur. Radiol.* **2014**, *24*, 1339–1348. DOI: 10.1007/s00330-014-3144-7
14. Kim, J. W.; Lee, C. H.; Kim, S. B.; Park, B. N.; Park, Y. S.; Lee, J.; Park, C. M. Washout Appearance in Gd-EOB-DTPA-Enhanced MR Imaging: A Differentiating Feature Between Hepatocellular Carcinoma with Paradoxical Uptake on the Hepatobiliary Phase and Focal Nodular Hyperplasia-Like Nodules. *J. Magn. Reson. Imaging* **2017**, *45*, 1599–1608. DOI: 10.1002/jmri.25493
15. Nagtegaal, I. D.; Odze, R. D.; Klimstra, D.; Paradis, V.; Rugge, M.; Schirmacher, P.; Washington, K. M.; Carneiro, F.; Cree, I. A.; WHO Classification of Tumours Editorial Board. The 2019 WHO Classification of Tumours of the Digestive System. *Histopathology* **2020**, *76*, 182–188. DOI: 10.1111/his.13975
16. Ferlicot, S.; Kobeiter, H.; Tran Van Nhieu, J.; Cherqui, D.; Dhumeaux, D.; Mathieu, D.; Zafrani, E. S. MRI of Atypical Focal Nodular Hyperplasia of the Liver: Radiology-Pathology Correlation. *A.J.R. Am. J. Roentgenol.* **2004**, *182*, 1227–1231. DOI: 10.2214/ajr.182.5.1821227
17. Grazioli, L.; Bondioni, M. P.; Haradome, H.; Motosugi, U.; Tinti, R.; Frittoli, B.; Gambarini, S.; Donato, F.; Colagrande, S. Hepatocellular Adenoma and Focal Nodular Hyperplasia: Value of Gadoxetic Acid-Enhanced MR Imaging in Differential Diagnosis. *Radiology* **2012**, *262*, 520–529. DOI: 10.1148/radiol.11101742
18. Nguyen, B. N.; Fléjou, J. F.; Terris, B.; Belghiti, J.; Degott, C. Focal Nodular Hyperplasia of the Liver: A Comprehensive Pathologic Study of 305 Lesions and Recognition of New Histologic Forms. *Am. J. Surg. Pathol.* **1999**, *23*, 1441–1454. DOI: 10.1097/00000478-199912000-00001
19. Miyayama, S.; Matsui, O.; Ueda, K.; Kifune, K.; Yamashiro, M.; Yamamoto, T.; Komatsu, T.; Kumano, T. Hemodynamics of Small Hepatic Focal Nodular Hyperplasia: Evaluation with Single-Level Dynamic CT During Hepatic Arteriography. *A.J.R. Am. J. Roentgenol.* **2000**, *174*, 1567–1569. DOI: 10.2214/ajr.174.6.1741567

Preprints (www.preprints.org) | NOT PEER-REVIEWED | Posted: 20 December 2023 doi:10.20944/preprints202312.1508.v1

Disclaimer/Publisher's Note: The statements, opinions and data contained in all publications are solely those of the individual author(s) and contributor(s) and not of MDPI and/or the editor(s). MDPI and/or the editor(s) disclaim responsibility for any injury to people or property resulting from any ideas, methods, instructions or products referred to in the content.